AUSTRALIAN JOURNAL OF BASIC AND APPLIED SCIENCES

ISSN:1991-8178 EISSN: 2309-8414
Journal home page: www.ajbasweb.com

Hydrothermal treatment of electrospun ZnO nanofibers and its photocatalytic properties

Raad S. Sabry

Al-Mustansiriyah University, science of collage, department of physics

Address For Correspondence:
Raad S. Sabry, Al-Mustansiriyah University, science of collage, department of physics
E-mail: raadphy_dr@yahoo.com

ARTICLE INFO

Article history:
Received 13 March 2016
Accepted 21 May 2016
Published 24 May 2016

Keywords:
Twinned hexagonal nanotubes, electrospinning, methylene blue

ABSTRACT

In this study, a new nanostructure that consists of zinc oxide (ZnO) was produced by the electrospinning process followed by a hydrothermal technique. First, Electrospun technique was used to fabricate 1D nanofibers of ZnO, Polyvinylpyrrolidone (PVP)/ zinc acetate nanofibers were electrospun using a solution containing PVP dissolved in ethanol and zinc acetate in distilled water were mixed together, followed by calcination at 500°C for 3hours to remove the polymer produced pure ZnO nanofibers (NFs) . The nanofibers strongly enhanced outgrowing of ZnO nanostructures when a specific hydrothermal technique was used, FESEM results show a net of fibers with diameters less than 100 nm and several micrometers in length of ZnO, after calcinations process, when this fibers treatments by hydrothermal in low molarity of zinc acetate (0.2 M) the product is ZnO NFs covered by ZnO nanoparticles (ZnO NFs-NPs). while in high molarity (0.4M) product novel nanostructure which is ZnO NFs covered by ZnO nanotubes (NTs), (ZnO NFs –NTs) with twinned hexagonal nanotubes, This structure were found to be highly effective photocatalysts, as indicated by the almost complete removal (more than 98%) of the model compound methylene blue in only 40min.

INTRODUCTION

One-dimensional (1D) nanostructures have been a subject of intensive research due to their unique properties and applications (Bin Ding Jianyong Yu, 2014; Sheng Xu and Zhong Lin Wang, 2011). Recently, synthesis of complex architectures with controlled shapes, sizes, and compositions based on 1D structure has triggered great interest due to these hierarchical structures may provide opportunities to exploit new phenomena and novel properties (Yinhua Li, *et al*., 2010). ZnO, with a wide band gap of 3.4eV, high electron mobility and exciton binding energy (~60meV) has many potential applications in optoelectronics (wang, z.l., 2007), nanogenerators (Zhong Lin Wang, *et al*., 2012), gas and chemical sensors (RaadSaadon, Osama AbdulAzeez, 2014), lithium ion batteries (Linlin Wang, *et al*., 2015), solar cells (Mahmoud Abdelfatah a,b,c,n *et al*., 2016) and photocatalysts (Daimei Chen, *et al*., 2014; Noh Soo Han, *et al*., 2016). The practical application of ZnO is determined by its properties which can be modulated by convert its morphology, because the Control of the morphology and size of particulate materials has received increased attention due to the fact they play very important roles in determining magnetic, Electrical, optical, and other properties (Linping Xu, *et al*., 2009), ZnO have wide range of nanostructurs morphologies such as nanoflowers, nanotubes, nanorods, nanobelts, nanowires (Yinhua Li, Jian Gong, Yulin Deng, 2010; Lingling Miao, *et al*., 2012).

These structures can be produced using various methods such as the CVD, sol-gel process (ZOHRA NAZIR KAYANI1 *et al*., 2015) pulse laser ablation (Raad, S. *et al*., 2015) thermal oxidation (Chia-Yen Hsu, *et al*., 2015) hydrothermal (Yung-Chun Tu, *et al*., 2015) electrospinning (Mohammad Sajad Sorayani Bafq, *et al*.,

To Cite This Article: Raad S. Sabry., Hydrothermal treatment of electrospun ZnO nanofibers and its photocatalytic properties. ***Aust. J. Basic & Appl. Sci.,*** *10(9): 307-314, 2016*

12015) and electrochemical deposition (Jennifer Torres Damasco Ty and Hisao Yanagi, 2015) Among these techniques pertaining to the 1D nano-materials, the electrospinning method is more versatile and convenient than the other processes for synthesizing of continuous fibers with diameters down to a few nanometers, which shares the characteristics of both electrospraying and conventional solution dry spinning. The method can be applied to synthetic and natural organic and inorganic, as well as to metals, metal oxides and ceramics nanofibers (Bin Ding Jianyong Yu, 2014; Jeong-Ha Baek, *et al*., 2012) One-dimensional ZnO nanostructures have attracted more attention because of its incomparable special performance, Also hydrothermal is one of the most common and promising methods for the synthesis of isometric ZnO crystals (Qi Qi, *et al*., 2008) this method have many advantages such as a one-step synthesis without any additional processes like catalyst or buffer layer (Kim Kang-Min), This solution-based technique has additional advantages; it is environmentally friendly, economical, and yields large quantities of monodisperse, well-aligned, and simple and low-cost method (Raad S. Sabry, Osama AbdulAzeez, 2014; Thushara, J. *et al*., 2013)

Unlike TiO_2, ZnO can be molded into various nanostructures by simply controlling the synthesis parameters. ZnO nanorods, nanotube and nanofibres provide high aspect ratio and direct conduction pathway for the rapid collection of photogenerated electrons (Thushara, J. *et al*., 2013).

In this study, we report a new ZnO nanofibers-nanotubes structure which was successfully prepared by the electrospun ZnO nanofibers as seed to guide hydrothermal growth of the ZnO nanotubes, the obtained nanofibers and the hierarchical nanostructure were then separately used as photocatalysts for degradation of methylene blue dye (MB).

Experimental:

1. Chemicals:

Polyvinylpyrrolidone (PVP) (MW=1,300,000 Sigma Aldrich,USA), zinc acetate dehydrate (ZnAc) $Zn(CH_3CO_2)_2.2H_2O$,(scharlau,spain), zinc nitrate hexahydrate ($Zn(NO_3)_2.6H_2O$), Scharlau, Spain), ethanol (99%scharlau, spain), Hexamethylenetetramine $C_6H_{12}N_4$ (HMT), (BDH), NaOH (99% scharlau,spain), deionized water DI, MB dihydrate (95.0 assay).

2. Fabrication of ZnO nanofibers:

To Preparation of the precursor solution by dissolving 6wt. % of PVP in ethanol, and zinc acetate solution by dissolving 40 wt. % in deionized water. Both solutions were stirred separately for 2 hour at room temperature. After that, 7.5 wt. % of zinc acetate solution was transferred to PVP solution with constant stirring for 2hours at room temperature. A viscous mixed solution of zinc acetate and PVP was obtained.

Finally, the viscous precursor solution was loaded to a plastic syringe connected to 21-gauge stainless steel needle was used as the nozzle. The feeding rate of the solution was adjusted by using syringe pump (KDS 200, USA) at a constant rate of 1ml/h. The emitting electrode from a Gamma High Voltage Research ES30P power supply capable of generating DC voltages up to 25 kV was attached to the needle. The grounding electrode from the same power supply was attached to a plate of aluminium with clean P-type Si substrates fixed on it which was used as the collector plate and was placed 18 cm in front of the tip of the needle When an applied voltage of 16 kV is subjected across the needle and the collective plate, a fluid jet was ejected from the nozzle as shown in figure 1, The resulting electrospun nanofibers were then collected and calcined at 500°C for 3 h,

3. Growth of ZnO nanotubes on ZnO nanofiber:

Zinc oxide nanotube structure was synthesis using hydrothermal method. (0.2 and 0.4M) of zinc nitrate hexahydrate and hexamethylenetetramine (HMT) were dissolved in 100 ml deionized water. Then, (0.2 M) of NaOH was added to the mixture under slow stirring for 1 hour at room temperature to adjust pH of solution using (BP3001Professional Benchtop pH Meter). The prepared solution was transferred to Teflon lined stainless steel autoclave then,The Si substrates coated with electrospun ZnO NFs was incontact with the bottom of the Teflon vessel ("face-down") and autoclave medium as shown in fig.1 after sealed the autoclave was heated to 110 °C for 5 hour in an oven. After that the autoclave cooled down to room temperature. The obtained white powder was washed several times by distilled water to remove residues and impurities.

X-ray diffraction (XRD) of the calcined ZnO NFs, ZnO NFs-NPs and ZnO NFs -NTs was conducted on a (miniflex II Rigaku, Japan) with Cu kα radiation. Field emission scanning electron microscopy (FE-SEM) images were recorded by (Hitachi-S 4160-Japan), UV- visible of the ZnO NFs, ZnO NFs-NPs and ZnO NFs -NTs recorded by using a Optima Sp-3000 plus UV-Vis-NIR (Split- beam Optics, Dual detectors) spectrophotometer.

4. Photocatalytic Degradation of methylene blue:

The photocatalytic activity of the prepared hierarchical ZnO was investigated by the degradation of a standard MB solution in a photochemical reactor. A 20 mg/L MB aqueous solution, which was prepared using distilled water, was employed as model pollutant to measure the photocatalytic activity of the ZnO catalysts.

Approximately 20 mg of ZnO photocatalytic powder was added into a quartz beaker containing 50 mL of MB aqueous solution. The solution was placed in a photocatalytic reactor and stirred in the dark for 80 min to ensure the establishment of adsorption and desorption equilibrium of MB on the ZnO surface. The suspension was subsequently irradiated with a UV lamp (λ = 366 nm; CAMAG company). At 40-min interval with gently stirred, 5 ml (for analysis every 10min) of the suspension was extracted and then centrifuged at 8000 rev/ min for 20 min to separate the powder from the supernatant. UV–Vis spectroscopy was used to generate time dependent absorbance changes in the supernatant between 400 and 800 nm. Color removal of the dye solution was determined by measuring the absorbance at λ = 664 nm with a UV–visible spectrophotometer, which was initially calibrated in accordance with Beer–Lambert's law. Figure 1 show a schematic diagram of synthesis the ZnO NFs, ZnO NFs-NPs and ZnO NFs-NTs and photocatalytic activity under UV light.

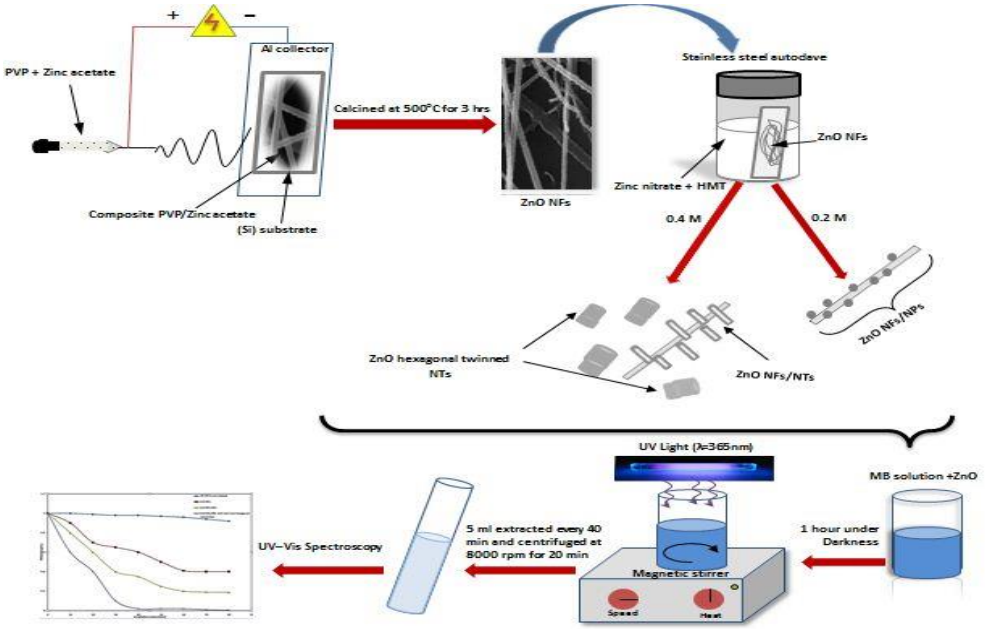

Fig. 1: Synthesis of ZnO NFs, ZnO NFs-NPs and ZnO NFs-NTs and photocatalytic activity measurements.

X-ray diffraction (XRD) of the calcined ZnO NFs, ZnO NFs-NPs and ZnO NFs-NTs was conducted on a (miniflex II Rigaku, Japan) with Cu kα radiation. Field emission scanning electron microscopy (FE-SEM) images were recorded by (Hitachi-S 4160-Japan), UV- visible of the ZnO NFs and ZnO NFs-NTs recorded by using a Optima Sp-3000 plus UV-Vis-NIR (Split- beam Optics, Dual detectors) spectrophotometer.

RESULTS AND DISCUSSIONS

Figure 2 shows the XRD pattern of uncalcined and calcined ZnO NFs, ZnO NFs-NPs and ZnO NFs-NTs in different molarities. The XRD patterns indicate that

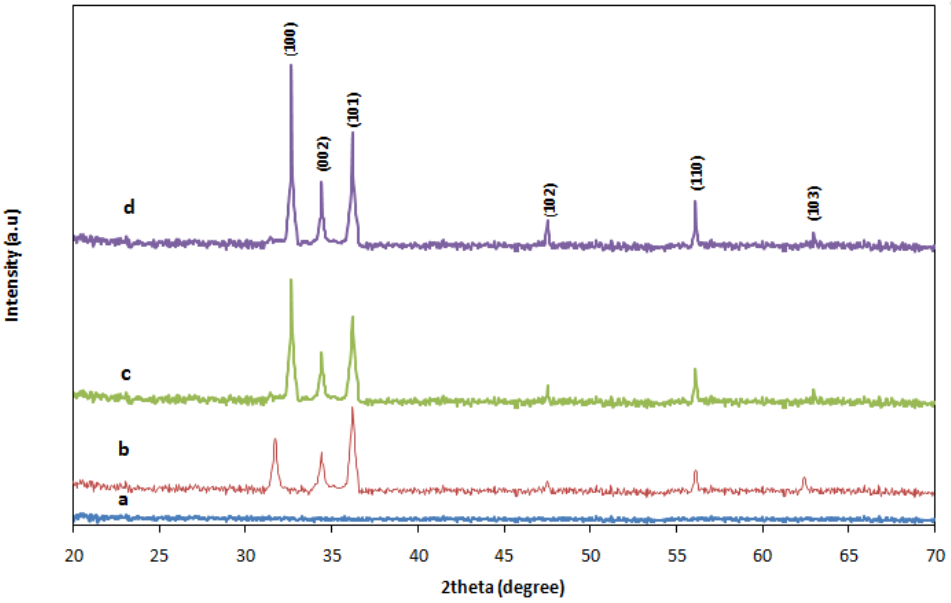

Fig. 2: XRD pattern of : (a) As electrospun uncalcined PVP-zinc acetate composite (b) after calcined at 500 °C (c) hydrothermal treatment in 0.2 M zinc acetate (d) hydrothermal treatment in 0.4 M zinc acetate.

uncalcined PVP-zinc acetate composite nanofibers were amorphous and had no obvious diffraction peaks Fig. (2-a). While the composite nanofibers were calcined at 500 °C the pattern of the samples shows obvious diffraction peaks. With the calcinations temperature rising, the diffraction peaks strengthened and the crystallinity became high. The spectra shows diffraction peaks at 31.74° (100),34.46°(002), 36.24° (101), 47.56° (102), 56.56° (110), 62.94° (103), All these diffraction peaks can be perfectly indexed as a typical hexagonal wurtzite structure of ZnO (JCPDS No.36-1451) No other diffraction peaks were detected, which indicates that there were no impurities present and the precursors had been completely transformed into ZnO. We can obverse that the diffraction from (101) plane is the strongest in ZnO nanofibers, while the diffraction from (100) plane of ZnO NFs-NPs and ZnO NFs-NTs becomes the strongest. This may be due to the preferential orientation of the epitaxial growth of ZnO NTs.

Crystallite sizes were calculated using Scherrer formula (Raad S. Sabry, Osama AbdulAzeez, 2014):

$D= k \lambda/(\beta \cos\theta)$

Where D is the crystallite size in nanometers, k is a constant (0.9, assuming that the particles are spherical), λ is the Wavelength of the X-ray radiation (CuKα = 0.1541 nm), β is the FWHM (full width at half maximum) of the strongest peak, and h is the diffraction angle. The crystallite sizes of the ZnO NFs were calculated using the diffraction peaks of the (101) crystalline plane while for ZnO NFs-NPs and ZnO NFs-NTs were calculated using the diffraction peaks of the (100) crystalline plane . The results showed that the crystallite sizes of the ZnO NFs is 13.85 while for ZnO NFs-NPs and ZnO NFs-NTs found to be 15.05, and 14.49 nm respectively.

Fig. (3a and b) shows FE-SEM images of the as prepared electrospun nanofiber mats that were prepared from ZnAc/PVP before and after calcinations, respectively. As can be clearly seen, smooth and continuous nanofibers formed after electrospinning of the prepared sol–gel. As observed, the length of the fibers can even reach the centimeter grade and have a diameter between (300) nm and (90) nm. The distributions of the nanofibers are continuous and fairly random that the surface of the composite ZnAc/PVP. the diameter of ZnO NFs after calcination process, are decrease to (~80) nm. This size reduction of the fibers is due to the removal of the PVP during the calcination process and the crystallization of ZnO.

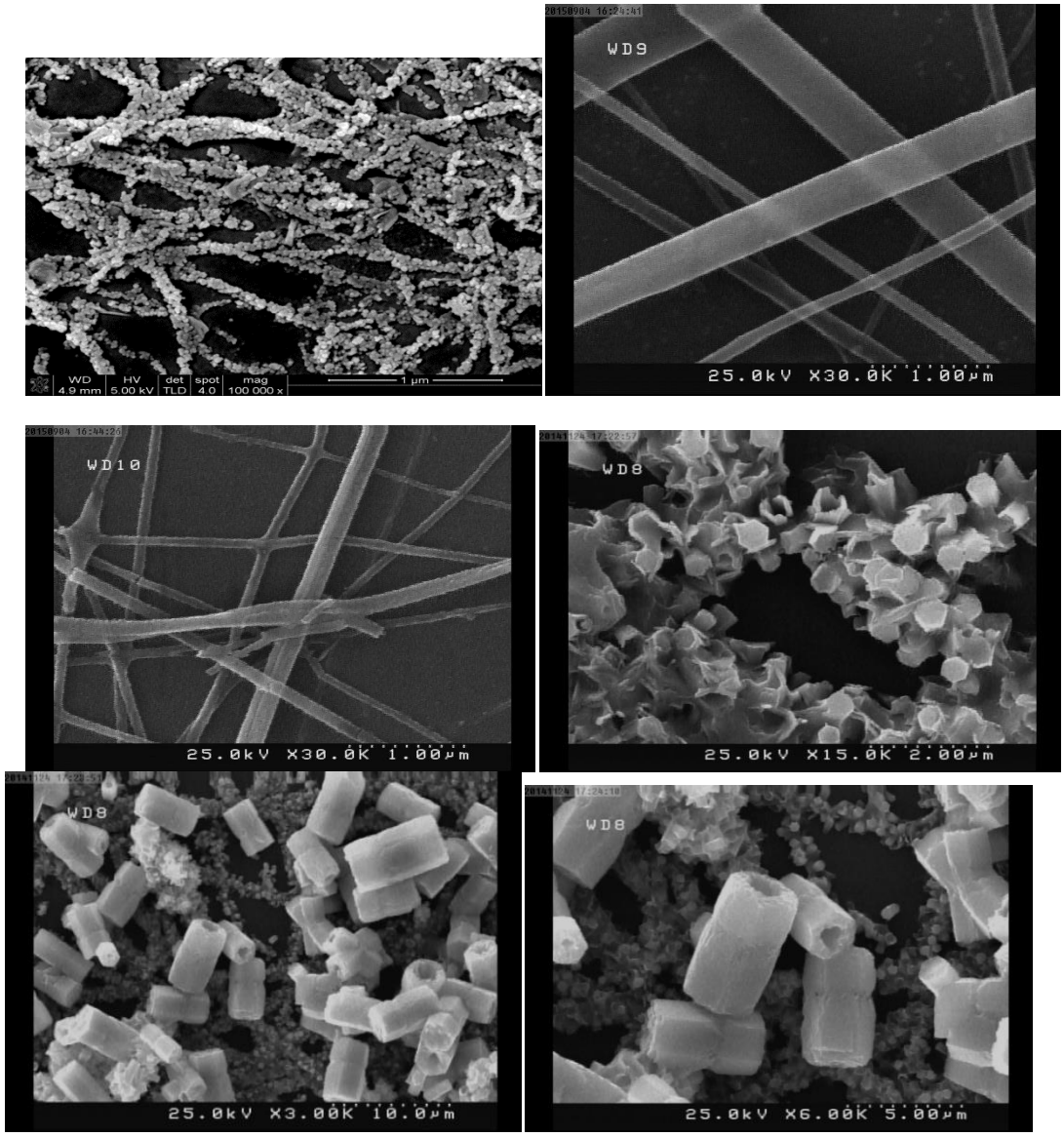

Fig. 3: FE-SEM images of (a) Zinc acetate / PVP composite NFs, and (b) ZnO NFs after calcination at 500°C,(C) ZnO NFs-NPs after hydrothermal treatment in (0.2 M), (d)) ZnO NFs-NTs after hydrothermal treatment in (0.4 M),(e) ZnO NFs-NTs and twinned hexagonal nanotubes, (f) high magnification of ZnO NFs-NTs and twinned hexagonal nanotubes

Fig. (3c) represents FE-SEM images of the ZnO NFs product by electrospun technique after calcinations and hydrothermal treatment in 0.2 M zinc nitrite solution, small outgrowths can be seen around the nanofibers that were obtained from the (ZnNPs) containing solution due to the hydrothermal treatment process. When increasing the morality of the zinc nitrite for hydrothermal treatment to 0.4 M dramatic change accrue, that's clear from FE-SEM image as shown in Fig. (3d) open and closed end hexagonal nanotubes completely outgrowths can be seen around the nanofibers, also its clear from Fig. (3 e and f) that twinned hexagonal nanotubes in different size were formed in high molarity (0.4M),Twinned structures are very commonly formed by wet chemical methods (Sheng Xu and Zhong Lin Wang, 2011; Poulomi Roy)

All hydrothermal reactions are actually in equilibrium and can be controlled by adjusting the reaction parameters, such as precursor concentration, growth temperature and growth time, pushing the reaction equilibrium forwards or backwards (Sheng Xu and Zhong Lin Wang, 2011), the formation of this twinned ZnO structures when at high precursor concentration(high molarity of zinc nitrate) used in hydrothermal can be explained as the excess in Zn^{2+} ions which with O^{2-} ions provided form H_2O in presence of HMTA (a nonionic cyclic tertiary amine), form more ZnO nanostructures.

The photocatalytic activity of prepared ZnO NFs, ZnO NFs-NPs and ZnO NFs-NTs were evaluated by Methyl blue dye degradation after exposure to UV light.

The photocatalytic mechanism of ZnO has been mentioned in many reports (Thushara, J. *et al*., 2013; Arshid M. Ali, *et al*., 2010), Due to the generation of positive holes and negative electrons, oxidation-reduction reactions take place at the surface of semiconductors which occur when the ZnO catalyst is excited under the irradiation of a UV lamp. In the oxidative reaction, the positive holes react with the moisture present on the surface and produce a hydroxyl radical.

An electron in an electron-filled valence band (VB) is excited by photoirradiation to a vacant conduction band (CB), leaving a positive hole in the VB. These electrons and positive holes will drive the reduction and oxidation, respectively, of compounds adsorbed on the surface of a photocatalyst. The activation equation can be written as (Du, P.F., *et al*., 2011):

$h\upsilon_{uv} + ZnO \longrightarrow ZnO\ (h^{+\ VB} + e^{-\ CB})$ (1)

In this reaction, h^+ and e^- are powerful oxidizing and reducing agents, respectively. The oxidation reactions can be expressed as:

$h^+ + H_2O \longrightarrow H^+ + \cdot OH$ (2)

$2h^+ + 2H_2O\cdot \longrightarrow 2H^+ + H_2O_2$ (3)

$H_2O_2 \longrightarrow HO\cdot + \cdot OH$ (4)

The reduction reactions can be expressed as:

$e^- + O_2 = \cdot O_2$ (5)

$\cdot O^-_2 + 2HO\cdot = H_2O_2 + O_2$ (6)

$HOOH = HO\cdot + \cdot OH$ (7)

Ultimately, the hydroxyl radicals are generated in both their actions. These hydroxyl radicals are very oxidative in nature and non selective with redox potential of E0 = +2.8.

Figure (4) shows the concentration changes of the MB dyes solution as a function of irradiation time of the photo degradation reactions over blank (without ZnO), ZnO NFs, ZnO NFs-NPs and ZnO NFs-NTs, The photodegradation efficiency for each experiment, also called conversion, was estimated by the following relationship and is shown in Fig(5):

$X\ \% = C0 - C/C_0 \times 100$ (10)

Where X is the photodegradation efficiency, C_0 is the concentration of MB before illumination, and C is the concentration of MB in the suspension after time t (mg/L).

In the case of blank, less than 8% of the dye was oxidized even after 80 min, when the catalyst ZnO NFs is employed; the samples exhibit good degradation efficiency. The degradation efficiency of the samples calcinated at 500 °C about 60% in 60min. as shown from the figure, when ZnO NFs-NPs are employed as catalyst its clear that the degradation efficiency of MB increased to about 80% in 60min,while in the case of ZnO NFs-NTs we note that the degradation efficiency of MB increased to about 85% in 35min more than 98% in only 40 min, In a study on TiO_2 photocatalyst, Ohtani *et al*. (Ohtani, B., *et al*., 1997) proposed a hypothesis, viz., a high photocatalytic activity of TiO_2 should depend on two factors: One is large specific surface area to absorb more target dye, the other is high crystallinity to minimize the recombination rate of photoinduced electron-hole pairs, According to these two facts we can explain our result,the good degradation efficiency of ZnO NFs become from the fact that the aspect ratio of the nanofibers is very high compare with other nanostructures which mean more absorb of the MB.

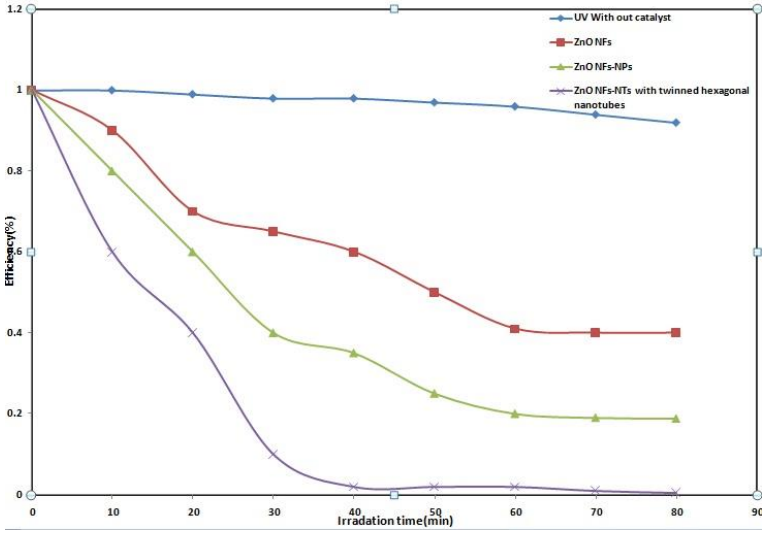

Fig. 4: Time-dependent photodegradation of MB under UV irradiation with and without synthesized ZnO photocatalyst

After hydrothermal treatments:

At the first case, (0.2M) concentration led to product ZnO NFs completely covered by ZnO NPs (ZnO NFs-NPs) that clear in FESEM results, this structures added more area to the surface of the fibers these rustle was agreement with other researches (Yinhua Li, Jian Gong, Yulin Deng, 2010; Lingling Miao, *et al*., 2012), also form XRD results shows that the crystallinity was improved which mean improving to degradation efficiency and reduces the degradation time, in the second case of 0.4 M which product

ZnO NFs-NTs which mean more are to the surface also the XRD results shows that the crystallinity was improved compare with low molarity. Now, from the FESEM results that clear that there are two types of nanotubs appeared, nanotubes covered the NFs (ZnO NFs-NTs) also twinned hexagonal nanotubes additive to the structures that mean, the ZnO nanotubes in addition to large surface areas and oxygen vacancies, which is very important in photocatayst activity so that the polar planes which is the most important things that effected on photocatayst activity. Wurtzite structure ZnO is a classic polar crystal. Thus, there are two types of wurtzite ZnO (0001) surface structures: Zn-polar surfaces with O-atom terminations and O-polar surfaces with Zn-atom terminations, these two polar surfaces have different properties (Olga Dulub, *et al*., 2003).

The morphology models of ZnO hexagonal nano tube, the top and bottom surface almost disappear, remaining $(10\bar{1}0)$ surfaces, Kislov *et al*. (Nikolai Kislov, *et al*., 2009) investigated that ZnO $(10\bar{1}0)$ surfaces exhibit highest photocatalytic activity, while ZnO crystal with O-$(000\bar{1})$ terminations and Zn-(0001) terminations surface shows the lowest photocatalytic activity (Nikolai Kislov, *et al*., 2009), from the explanation mentioned above it can be concluded that our experimental results shows that the two types ZnO NFs-NTs plus twinned hexagonal have the best and unique characteristics photocatalytic activity than other nanostructures.

Conclusions:

ZnO NFs, ZnO NFs-NPs structures and a novel structures of ZnO NFs-NTs was obtained with high surface area was successfully prepared by very simple and low coast methods, the combination of electrospinning method and hydrothermal reaction. The XRD results indicate that ZnO NFs-NTs have high crystallinity with a hexagonal wurtzite structure.FESEM results shows that when increase the molarty the ZnO NFs from ZnO NFs-NPs to ZnO NFs-NTs with twinned hexagonal nanotubes, this novel structure was dramatic improve the photocatalytic activity of MB where more than 98% of the dye was vanished in only 40 min irradiation time,The results strongly recommend exploiting the synthesized ZnO NFs-NTs with twinned hexagonal nanotubes as a super active photocatalyst.

REFERENCES

Bin Ding Jianyong Yu, 2014.Electrospun Nanofibers for Energy and Environmental Applications, Springer-Verlag Berlin Heidelberg.

Sheng Xu and Zhong Lin Wang, 2011. One-Dimensional ZnO Nanostructures: Solution Growth and Functional Properties, Nano Res., 3(9): 676–684 ISSN 1998-0124 DOI 10.1007/s12274-011-0160-7.

Yinhua Li, Jian Gong, Yulin Deng, 2010. Hierarchical structured ZnO nanorods on ZnO nanofibers and their photoresponse to UV and visible lights, Sensors and Actuators A 158: 176-182.

wang, z.l., 2007. Novel nanostructures of ZnO for nanoscale photonics, optoelectronics, piezoelectricity, and sensing, Appl. Phys. A.

Zhong Lin Wang, Guang Zhu, Ya Yang, Sihong Wang, and Caofeng Pan, 2012. progress in nanogenerators for portable electronics, materials today | VOLUME 15 | NUMBER 12, DECEMBER.

RaadSaadon, Osama AbdulAzeez, 2014. Chemical Route to Synthesis Hierarchical ZnO Thick Films for Sensor Application, Energy Procedia, 50: 445-453.

Linlin Wang, Kaibin Tang, Min Zhang1 and Jingli Xu1, 2015. Facile Synthesis of Mn-Doped ZnO Porous Nanosheets as Anode Materials for Lithium Ion Batteries with a Better Cycle Durability, Nanoscale Research Letters, 10: 280.

Mahmoud Abdelfatah a,b,c,n, Johannes Ledig a,c, AbdelhamidEl-Shaer b, AlexanderWagner a, VicenteMarin-Borras d, AzatSharafeev e, PeterLemmens c,e, Mohsen Mohamed Mosaad b, Andreas Waag a,c, Andrey Bakin, 2016. Fabricationandcharacterizationoflowcost Cu2O/ZnO:Al solarcells for sustainablephotovoltaicswithearthabundantmaterials, Solar Energy Materials & Solar Cells, 145: 454-461.

Daimei Chen, Zhihong Wang, Tiezhen Ren, Hao Ding, Wenqing Yao, Ruilong Zong and Yongfa Zhu, 2014. Influence of Defects on the Photocatalytic Activity of ZnO, XXXX American Chemical Society.

Noh Soo Han, Dukhan Kim, Jong Woon Lee, Jaehyun Kim, Hyeong Seop Shim, Yongjin Lee, Dongil Lee, and Jae Kyu Song, 2016. Unexpected Size Effect Observed in ZnO-Au Composite Photocatalysts, ACS Appl. Mater. Interfaces.

Linping Xu, Yan-Ling Hu, Candice Pelligra, Chun-Hu Chen, Lei Jin, Hui Huang, Shanthakumar Sithambaram, Mark Aindow, Raymond Joesten and Steven L. Suib, 2009. ZnO with Different Morphologies Synthesized by Solvothermal Methods for Enhanced Photocatalytic Activity, Chem. Mater., 21: 2875-2885 287.

Lingling Miao, Haiming Zhang, Yanjun Zhu,Yan Yang,Qin Li,Jing Li, 2012. Epitaxial growth of ZnO nanorods on electrospun ZnO nanofibers by hydrothermal method, J Mater Sci: Mater Electron, 23: 1887-1890.

ZOHRA NAZIR KAYANI1_, MARYAM IQBAL1, SAIRA RIAZ2, REHANA ZIA1, SHAHZAD NASEEM2, 2015. Fabrication and properties of zinc oxide thin film prepared by sol-gel dip coating method, Materials Science-Poland, 33(3): 515-520.

Raad, S. Sabry, Asaad M. Abbas, Firas S. Mohammed,Wisam J. Aziz1, 2015. Novel method to transform ZnO nanorods into interlaced tattered nanosheets by changing the target inclination angle, J Mater Sci: Mater Electron.

Chia-Yen Hsu,a Kai-Hsiang Chang,a Jyun-An Gong,b Jonas Tir´en,c Yuan-Yao Li abd and Akiyoshi Sakoda, 2015. Kirkendall void formation and selective directional growth of urchin-like ZnO/Zn microspheres through thermal oxidation in air, RSC Adv., 5: 103884.

Yung-Chun Tu,Shui-Jinn Wang, Tseng-Hsing Lin, Chien-Hsiung Hung,Tsung-Che Tsai,1 Ru-Wen Wu,1 Kai-Ming Uang,3 and Tron-Min Chen, 2015. Hydrothermal Growth of Quasi-Monocrystal ZnO Thin Films and Their Application in Ultraviolet Photodetectors, Hindawi Publishing Corporation International Journal of Photoenergy, Article ID 261372, 7.

Mohammad Sajad Sorayani Bafq, Roohollah Bagherzadeh and Masoud Latifi1, 2015. Fabrication of composite PVDF-ZnO nanofiber mats by electrospinning for energy scavenging application with enhanced efficiency, J Polym Res., 22: 130.

Jennifer Torres Damasco Ty and Hisao Yanagi, 2015. Electrochemical deposition of zinc oxide nanorods for hybrid solar cells, Japanese Journal of Applied Physics, 54: 04DK05.

Jeong-Ha Baek, Juyun Park, Jisoo Kang, Don Kim, Sung-Wi Koh and Yong-Cheol Kang, 2012. Fabrication and Thermal Oxidation of ZnO Nanofibers Prepared via Electrospinning Technique, Bull. Korean Chem. Soc., 33: 8.

Qi Qi, Zhang Tong, Liu Li, Zheng Xuejun, Yud Qingjiang, Zheng Yi. 2008. Selective acetone sensor based on dumbbell-like ZnO with rapidresponse and recovery. Sens Actuators B; 134: 166-70.

Kim Kang-Min, Kim Hae-Ryong, Choi Kwon-Il, Kim Hyo-Joong, Lee Jong-Heun. ZnO hierarchical nanostructures grown at room temperature and their C2H5OH sensor applications. Sens Actuators B., 155: 745-51.

Raad S. Sabry, Osama AbdulAzeez, 2014. Hydrothermal growth of ZnO nano rods without catalysts in a single step, Manufacturing Letters, 2: 69-73.

Thushara, J. Athauda, Umaiz Butt, Ruya R. Ozer, 2013. Hydrothermal growth of ZnO nanorods on electrospun polyamide nanofibers, MRS Communications, 3: 51-55.

Poulomi Roy, Kamalesh Mondal, and Suneel K. Srivastava, Synthesis of Twinned CuS Nanorods by a Simple Wet Chemical Method, Crystal Growth & Design, 8: 5.

Arshid M. Ali, Emma A.C. Emanuelsson, Darrell A. Patterson, 2010. Photocatalysis with nanostructured zinc oxide thin films: The relationship between morphology and photocatalytic activity under oxygen limited and oxygen rich conditions and evidence for a Mars Van Krevelen mechanism, Applied Catalysis B: Environmental, 97: 168-181.

Du, P.F., L.X. Song, J. Xiong, Z.Q. Xi, J.J. Chen, L.H. Gao and N.Y. Wang, 2011. High-Efficiency Photocatalytic Degradation of Methylene Blue Usin Electrospun ZnO Nanofibers as Catalyst, Journal of Nanoscience and Nanotechnology, 11: 7723–7728.

Ohtani, B., Y. Ogawa and S.I. Nishimoto, 1997. Photocatalytic Activity of Amorphous-Anatase Mixture of Titanium(IV) Oxide Particles Suspended in Aqueous Solutions J. Phys. Chem. B 101: 3746.

Olga Dulub, Ulrike Diebold, and G. Kresse, 2003. Novel Stabilization Mechanism on Polar Surfaces: ZnO(0001)-Zn, PH YSICA L R EV I EW L ET T ERSVOLUME 90, NUMBER 1 10.

Nikolai Kislov, Jayeeta Lahiri, Himanshu Verma, D. Yogi Goswami, 2009. Elias Stefanakos, and Matthias Batzill, Photocatalytic Degradation of Methyl Orange over Single Crystalline ZnO: Orientation Dependence of Photoactivity and Photostability of ZnO, Langmuir, 25: 3310-3315.